THE JOURNAL OF PHYSICAL CHEMISTRY Letters

Letter

Cite This: J. Phys. Chem. Lett. 2018, 9, 2956−2960

pubs.acs.org/JPCL

Dynamics of Phospholipid Membranes beyond Thermal Undulations

Sudipta Gupta,*[,†] Judith U. De Mel,[†] Rasangi M. Perera,[†] Piotr Zolnierczuk,[‡] Markus Bleuel,[§] Antonio Faraone,[§] and Gerald J. Schneider*[,†,∥]

[†]Department of Chemistry, Louisiana State University, Baton Rouge, Louisiana 70803, United States

[‡]Jülich Centre for Neutron Science (JCNS), Outstation at SNS, POB 2008, 1 Bethel Valley Road, Oak Ridge, Tennessee 37831, United States

[§]NIST Center for Neutron Research, National Institute of Standards and Technology, Gaithersburg, Maryland 20899-6100, United States

[∥]Department of Physics & Astronomy, Louisiana State University, Baton Rouge, Louisiana 70803, United States

Supporting Information

ABSTRACT: We investigated the molecular dynamics of unilamellar liposomes by neutron spin echo spectroscopy. We report the first experimental evidence of a short-range motion at the length scale of the size of the headgroup of a lipid. The associated mean squared displacement shows a $t^{0.26}$ dependence in the pico- to nanosecond region that indicates another process beyond the predictions of the Zilman−Granek (ZG) model ($t^{0.66}$) and translational diffusion (t^{1}). A comparison with theory shows that the observed low exponent is associated with a non-Gaussian transient trapping of lipid molecules in a local area and supports the continuous time random walk model. The analysis of the mean squared displacement leads to the important conclusion that the friction at the interface between water and liposomes plays a minor role. Center of mass diffusion of liposomes and transient trapping of lipids define the range in which the ZG model can be applied to analyze membrane fluctuations.

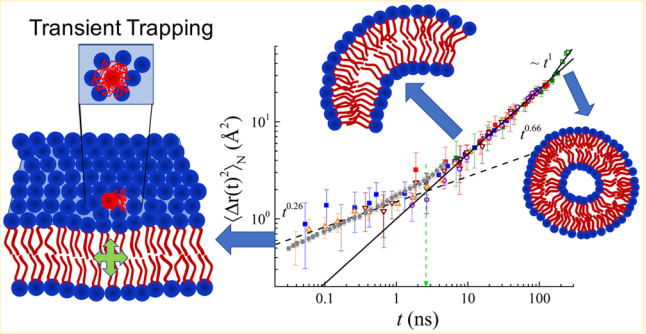

Phospholipids are an integral part of cell membranes in living cells and are ubiquitous in nature. Following their widespread applications in agriculture, food processing, and pharmaceuticals, deeper understanding of the structure and dynamics of membranes is essential.[1] Phospholipids with a hydrophilic head and a hydrophobic tail spontaneously self-assemble in aqueous media to form liposomes. The lipid bilayers appear to be a three-dimensional continuous closed vesicle where the shape fluctuations on a nanosecond time scale depend on the bending modulus of the membrane.[2,3] The bending mechanism is related to important biological functioning like cellular uptake and release.[4] Considering an ensemble of membrane plaquettes at random orientations, Zilman and Granek were successful in estimating the bending stiffness to describe the thermal membrane undulations.

However, the closest packing of lipid molecules causes a viscoelastic and heterogeneous behavior, which leads to the random anomalous diffusion observed in living cell membranes, and their molecular dynamics is far from understood.[5−9] The origin of such anomalous motions is controversial. Different models have been proposed, which try to identify the most biologically relevant mechanisms, like the continuous time random walk (CTRW) model that assumes transient trapping of lipids[10] and fractional Brownian motion (FBM) model that accounts for geometrical inhomogeneities in lipid bilayers.[11] Such motions in the bilayers are supposed to be coupled to the overall vesicle dynamics at appropriate length and time scales, and a proper exploration of the anomalous motions in lipid bilayers is crucial to understand diffusion-limited reactions, signaling, and regulatory process in biomacromolecules.[12,13]

Neutron spin echo (NSE) spectroscopy has proven to be a powerful tool to follow the molecular motions in liposomes.[2,3,14] In this Letter, we use NSE to explore the molecular processes in lipid bilayers. As a major result of our study, we find evidence for local trapping and non-Gaussianity in the motion of lipids at the time-scale from picoseconds to nanoseconds, which strongly supports the CTRW model. Additionally, we identify the time region between the fast-local trapping and the slower center of mass diffusion of liposomes in which the Zilman−Granek (ZG) model accurately describes the experimental data and reveal that the energy dissipation between the membranes and the solvent plays a lesser role in the case of liposomes than in the case of objects with a lower bending modulus and single interfaces, like in microemulsions.

We studied the dynamics of 1,2-dioleoyl-*sn*-glycero-3-phosphocholine (DOPC) at 20 °C and compare the results

Received: April 2, 2018
Accepted: May 12, 2018
Published: May 12, 2018

DOI: 10.1021/acs.jpclett.8b01008
J. Phys. Chem. Lett. 2018, 9, 2956−2960

with those of other phospholipids, such as, 1,2-distearoyl-*sn*-glycero-3-phosphocholine (DSPC) at 65 °C, 1,2-dimyristoyl-*sn*-glycero-3-phosphocholine (DMPC) at 37 °C, and L-α-phosphatidylcholine (SoyPC) at 30 °C. These different temperatures are necessary to compare all of the liposomes in their respective fluidlike phases.

We used small-angle neutron scattering (SANS) and cryo-transmission electron microscopy (cryo-TEM) to characterize the static structure. NSE and dynamic light scattering (DLS) were used to study dynamics. A more detailed description is omitted here but can be found in the Supporting Information.

A simple approach to analyze the intermediate scattering function, $S(Q,t)$, as determined by NSE experiments, uses the Zilman−Granek model that introduces the bending rigidity to describe the membrane dynamics[15]

$$\frac{S(Q,t)}{S(Q)} = \exp[-(\Gamma_Q t)^{2/3}] \tag{1}$$

The only free parameter is the Q-dependent decay rate, Γ_Q, from which we derive the intrinsic bending modulus, κ_η, by[14,16,17]

$$\frac{\Gamma_q}{Q^3} = 0.0069\gamma\frac{k_BT}{\eta}\sqrt{\frac{k_BT}{\kappa_\eta}} \tag{2}$$

Here η is the viscosity; k_B the Boltzmann constant; T the temperature; and γ a weak, monotonously increasing function of κ_η/k_BT.[15] In the case of lipid bilayers, usually $\kappa_\eta/k_BT \gg 1$, leading to $\gamma = 1$.[2,14,15,17,18] Equation 2 can be derived from a modified ZG theory that includes intermonolayer friction. A detailed discussion is omitted here but can be found in the literature.[14,16,17]

In addition, the contribution of the translational center of mass diffusion, D_t, of the liposomes needs to be included in the analysis of the dynamic structure factor, and we rewrite eq 1 as[14,19]

$$\frac{S(Q,t)}{S(Q)} = \exp(-D_tQ^2t)\exp[-(\Gamma_q t)^{2/3}] \tag{3}$$

by assuming ZG motion and center of mass diffusion are statistically independent. The separate measurement of D_t by DLS avoids additional free parameters.

Figure 1a displays $S_{DLS}(Q,t)$ by DLS on DOPC. The corresponding hydrodynamic radius was found to be R_h = 664 ± 20 Å at a lipid mass fraction ϕ_w = 0.25%. The size distribution is presented in the inset with the corresponding log-normal polydispersity of 38 ± 2%. Figure 1b shows SANS data for ϕ_w = 0.25% and 5% samples. After the intensities are divided by the respective volume fractions, the intensity values at the two different concentrations are virtually identical, particularly in the Q range where we studied the dynamic correlation function by NSE (highlighted area). A more detailed inspection of the SANS data by a core−shell model adapted for liposomes[20] yields a perimeter radius of 536 ± 2 Å and a bilayer thickness of 36 ± 1 Å. Using a Schulz distribution or a log-normal distribution for the radius polydispersity yields 30 ± 2%. Cryo-TEM suggests a radius of ≈ 550 Å (inset of Figure 1b). Within the experimental uncertainties, the values of the diameters are consistent and agree very well with those reported in the recent literature.[14]

Our SANS analysis yields the total number of lipids per liposome, $n_L = (9.9 \pm 0.2) \times 10^4$. This number corresponds to

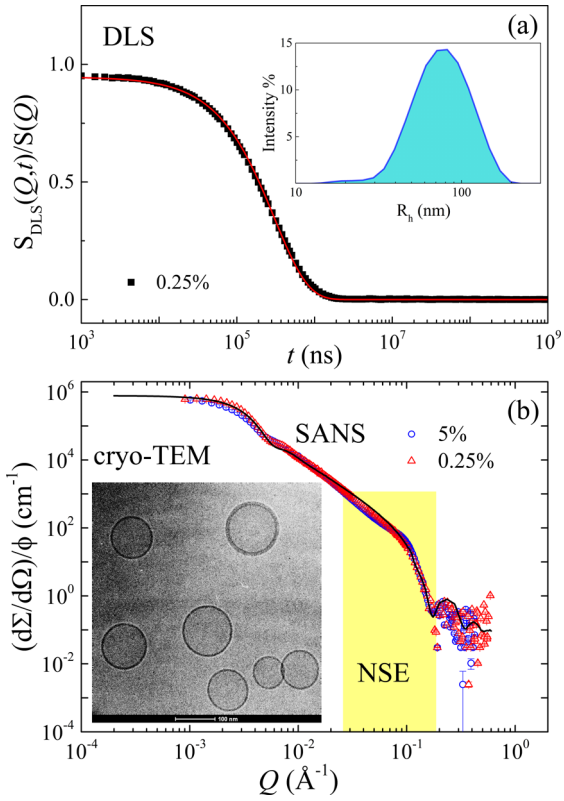

Figure 1. (a) Dynamic structure factor, $S_{DLS}(Q,t)/S(Q)$, from DLS autocorrelation function as a function of time. (b) SANS scattering intensity for ϕ_w = 5% and 0.25% DOPC dispersed in D_2O. Here, and throughout the paper, error bars in the figures and uncertainties in the text represent one standard deviation. The solid line represents the vesicle form factor. Inset: cryo-TEM image.

an average area per lipid of a = 69 ± 2 Å^2, which matches the value reported in the literature.[21]

Figure 2 illustrates $S(Q,t)$ by NSE in the fluid phase for ϕ_w = 1% and 5% DOPC samples. Using eq 1 and $\eta = \eta_{D_2O}$, we obtain the solid lines and $\kappa_{\eta,1}/(k_BT)$ = 20 ± 3 and 20 ± 2 for ϕ_w = 1 and 5%, respectively. Stimulated by earlier work,[14,19] we test the consequence of taking into account a finite diffusion coefficient, separately determined by DLS. The fits by eq 3 (dashed lines in Figure 2) can hardly be distinguished from the previous case and yield $\kappa_{\eta,2}/(k_BT)$ = 53 ± 5 and 44 ± 3 > $\kappa_{\eta,1}/(k_BT)$. These $\kappa_{\eta,2}/(k_BT)$ values disagree with typical values $\kappa_\eta \approx 20\ k_BT$, reported for large unilamellar vesicles (LUVs), DOPC, and other phospholipids.[2,22−24]

To identify the source of this contradiction, we now consider the local dissipation of the membrane fluctuation energy at the membrane−solvent interface, similarly to the analysis of NSE on microemulsions.[25] Therefore, we used the effective solution viscosity, $\eta = \eta_{D_2O+liposome}$, in eq 2 and recalculated κ_η. This leads to $\kappa_{\eta,3}/(k_BT)$ = 9 ± 1 (1% and 5%) for $\eta = \eta_{D_2O}$ (in eq 2) and $\kappa_{\eta,4}/(k_BT)$ = 22 ± 3 and 19 ± 2 for 1% and 5% respectively, for $\eta = \eta_{D_2O+liposome}$. While one value appears to be too low, the other seems to reflect the literature. Hence, the analysis appears to be ambiguous and deserves further attention. This becomes even more obvious if we vary the diffusion coefficient in our analysis, up to higher values found by PFG-NMR (Figure 3).[26] We also include the value of κ_η for the 0.1% sample reported from the literature.[14] The horizontal line represents 20 k_BT.

DOI: 10.1021/acs.jpclett.8b01008
J. Phys. Chem. Lett. 2018, 9, 2956−2960

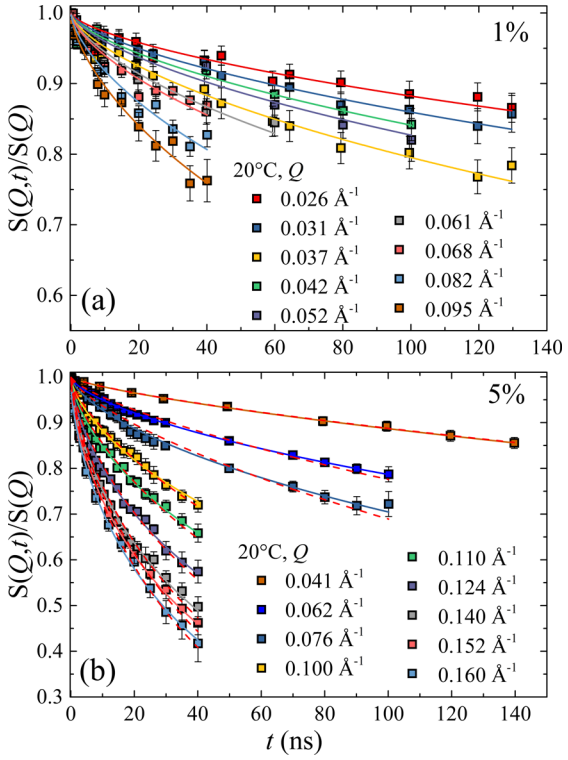

Figure 2. Dynamic structure factor, $S(Q,t)/S(Q)$, as a function of Fourier time, t, for different Q's as indicated for (a) 1% and (b) 5% samples. The solid and the dashed lines represent the fits using eqs 1 and 3, respectively.

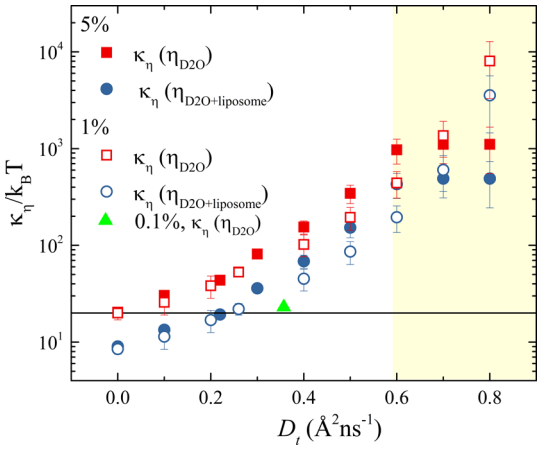

Figure 3. Intrinsic bending modulus, $\kappa_\eta/(k_BT)$, calculated for different translational diffusion, D_t, using the solvent viscosity, η_{D_2O}, or the measured solution viscosity, $\eta_{D_2O+liposome}$, for the viscosity, η, used in eq 2.

The apparent saturation and high uncertainty for $D_t \geq 0.6$ Å^2 ns^{-1} are due to the fact that the model fails to describe $S(Q,t)$ for large D_t (highlighted area) (see the Supporting Information). Figure 3 suggests a general trend depicting an exponential increase into unphysically large values of κ_η. The 0.1% sample is not affected, because in this case $\eta_{D_2O+liposome} \approx \eta_{D_2O}$ and there the measured solution viscosity is identical to the solvent viscosity.

To resolve this issue, hereafter, we calculate the mean squared displacement ($\langle \Delta r(t)^2 \rangle$, MSD) from $S(Q,t)$ and find a correct and nonambiguous answer that η_{D_2O} is correct, as has been previously used by numerous studies.[27,28] In addition, we reveal another process that can be associated with non-Gaussian transient trapping of lipid molecules predicted by molecular dynamics simulations at very short times.[29] Both diffusion and transient trapping define the range in which the ZG model can be used to analyze membrane fluctuations.

We used a cumulant expansion to obtain $\langle \Delta r(t)^2 \rangle$ and the non-Gaussianity parameter, $\alpha_2(t) = \frac{d}{d+2}\frac{\langle \Delta r(t)^4 \rangle}{\langle \Delta r(t)^2 \rangle^2} - 1$, which is defined by the quotient of the fourth $\langle \Delta r(t)^4 \rangle$ and the second moment squared $\langle \Delta r(t)^2 \rangle^2$ and $d = 3$, the dimension in space (Figure 4).[27,30]

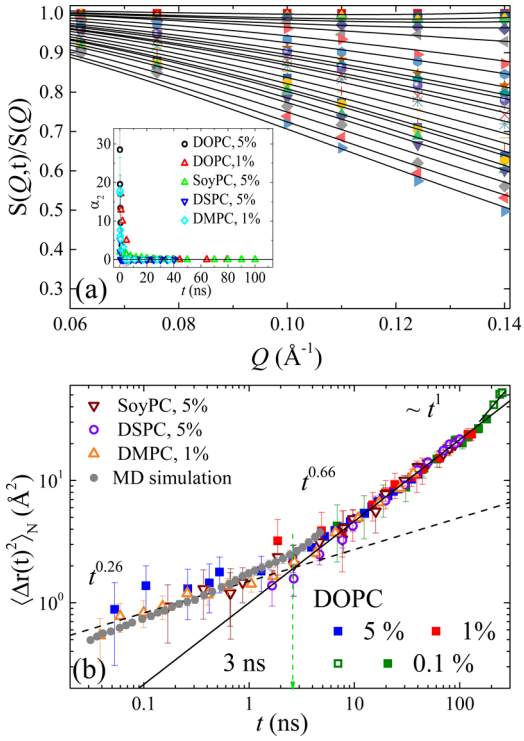

Figure 4. (a) Dynamic structure factor, $S(Q,t)$, as a function of Q for 5% DOPC, at 20 °C in D_2O for different Fourier times ranging from 0.05 to 40 ns (top to bottom). Inset, the non-Gaussian parameter for DOPC, DSPC, DMPC, and SoyPC samples. (b) The normalized mean squared displacement $\langle \Delta r(t)^2 \rangle_N$ versus Fourier time, t, calculated for 0.1%, 1%, and 5% DOPC; 10% DSPC; 1% DMPC; and 5% SoyPC samples. The data for 0.1% DOPC and 1% DMPC are calculated using $S(Q,t)/S(Q)$ from literature.[14,31] The solid and dashed lines represent the experimental power-law dependence, and filled circles are from MD simulation of POPE.[29]

Figure 4a exemplifies the extraction of $\langle \Delta r(t)^2 \rangle$ from the normalized dynamic structure factor, $S(Q,t)/S(Q)$, of DOPC with ϕ_w = 5%. The inset reports a Gaussian behavior for $t > 3$ ns but a non-Gaussian behavior for $t < 3$ ns. For the sake of a better comparability, we plotted the MSD normalized to the ZG contribution (Figure 4b). The original data can be found in the Supporting Information. We added different concentrations and different phospholipids to accomplish a more comprehensive picture, including 0.1% DOPC,[14] 1% DMPC,[31] 5% DSPC, and 5% SoyPC, all in the fluid phase.

In Figure 4, we identify three regions that can be distinguished by different power laws ($\cong t^n$). While the center

DOI: 10.1021/acs.jpclett.8b01008
J. Phys. Chem. Lett. 2018, 9, 2956−2960

of mass diffusion (t^1) is almost outside the observation window (open squares), the intermediate region exhibits $t^{0.66 \pm 0.01}$, and at low Fourier times ($t < 3$ ns), we find $t^{0.26 \pm 0.03}$. The time window, $3 \lesssim t \lesssim 180$ ns, for the $t^{0.66 \pm 0.01}$ region seems to be independent from the concentration and from the chemical composition of the lipids. The contribution of the center of mass diffusion of the liposomes shifts out of the observation window of the NSE for higher concentrations.

Flenner at al.[32] observed very rich dynamics in phospholipids, a ballistic motion, indicated by the t^2, at the fast time scale, and a subdiffusive $t^{0.67}$ (whole lipid) or $t^{0.43}$ (carbons in the tail) at the intermediate time scale. The motion in the intermediate time range corresponds to the so-called thermal undulations specified by the ZG model and the anomalous diffusion predicted by Monte Carlo simulations.[15,33] At the slow time scale, Flenner et al.[32] report a t^1 behavior, which is associated with the diffusion of lipids.

To associate it to our observations, let us compile some of the relevant facts, to discuss the lower exponent ($t^{0.26 \pm 0.03}$) for t $\lesssim$ 3 ns: (i) The length-scale associated with our observation window is 6 Å $\lesssim \sqrt{\langle \Delta r(t)^2 \rangle} \lesssim$ 14 Å, for 20 ps $\lesssim$ t $\lesssim$ 3 ns. (ii) The dynamics becomes non-Gaussian for $t < 3$ ns and α_2 increases with decreasing time. (iii) In agreement with the values reported in the literature, we determined the thickness of the bilayer, t_b = 36 Å.[2,34] The thickness of the bilayer in concert with the MSD shows that the corresponding dynamics occurs at the length-scale of single lipids and is faster than the anomalous diffusion in the ZG regime. (iv) The area per lipid is 69 ± 2 Å^2 for DOPC, which leads to an estimate of the perimeter radius $\approx$ 5 Å $\lesssim \sqrt{\langle \Delta r^2(3\text{ ns}) \rangle}$. Therefore, the motion is very local, which excludes a (hindered) diffusive motion of the liposomes at this time and length scale. This also excludes the by far slower flip-flop, rotational, and lateral diffusion mechanisms.[35] (v) Two theoretical frameworks are available to account for an exponent that is on the order of 0.3: (a) Fractional Brownian motion (FBM) as an expansion of the Brownian diffusion. A so-called anticorrelation causes the exponent of $\approx$ 0.3 within the FBM model.[29] However, this model is incompatible with the observed non-Gaussian behavior.[10,29] (b) The continuous time random walk (CTRW) model assumes a random-walk-like motion, but with random trapping times. It predicts subdiffusion and non-Gaussianity.[10,29] Our experimental results favor therefore the CTRW model. (vi) Molecular dynamics (MD) simulations of a palmitoyl-oleoyl-phosphatidylethanolamine (POPE) lipid bilayer suggest a fluctuation-like motion, including a finite non-Gaussianity for $t < 3$ ns, associated with the transition from a $t^{0.7}$ to $t^{0.33 \pm 0.02}$ power law at $t \approx 3$ ns with decreasing time.[29] (vii) Our experimental observations seem to be independent of the specific lipid. Therefore, we include the results of MD simulations in Figure 4 and find a surprisingly good agreement. The MD simulations show that lipids are caught in an area $\lesssim$ 7 Å × 7 Å, even at a longer time of up to 20 ns.[29] In the experiments, the contribution of the membrane undulations to the MSD becomes stronger for $t > 3$ ns and hides that of the lateral lipid motion. Thus, the simulations are well compatible with the experiments. From the simulations, we know that the low exponent is a consequence of the divergence of the mean trapping time, which naturally involves a non-Gaussian behavior. In other words, we identified a new region which corresponds to a lateral motion of lipids, which are trapped within a certain range that is on the order of the size of the molecule. The MD simulations and mode-coupling theory calculations by Flenner et al.[32] suggest that our experimental observation of a trapped motion is associated with the motion of the carbon tail of the fatty acid.

Our results have important consequences: (i) The analysis of the ZG membrane undulation is valid only in a certain time range. In our case, it is constrained by the transient trapping of the lipids on the one side and by the center of mass diffusion of the liposomes on the other side. (ii) Depending on the time range of the experiment, the center of mass diffusion can substantially change $S(Q,t)$. (iii) The MSD tells us whether the diffusion needs to be included in the analysis. Therefore, we can analyze the data accordingly and find that only the case $\eta = \eta_{D_2O}$ yields a correct description of the experimental data, which justifies the procedure that has been used in numerous cases.[2,3,17,31] (iv) Item iii implies that the local dissipation of the membrane fluctuation energy at the interface with the surrounding solvent plays a lesser role than in microemulsions.

■ ASSOCIATED CONTENT

Supporting Information

The Supporting Information is available free of charge on the ACS Publications website at DOI: 10.1021/acs.jpclett.8b01008.

Experimental methods and additional data (Figures S1−S5 and Table S1) (PDF)

■ AUTHOR INFORMATION

Corresponding Authors

*E-mail: g.sudipta26@gmail.com
*E-mail: gjschneider@lsu.edu

ORCID

Sudipta Gupta: 0000-0001-6642-3776
Antonio Faraone: 0000-0002-3783-5816

Notes

The authors declare no competing financial interest.

■ ACKNOWLEDGMENTS

The neutron scattering work is supported by the U.S. Department of Energy (DOE) under EPSCoR Grant No. DE-SC0012432 with additional support from the Louisiana Board of Regents. Access to the neutron spin echo spectrometer and small-angle scattering instruments was provided by the Center for High Resolution Neutron Scattering, a partnership between the National Institute of Standards and Technology and the National Science Foundation under Agreement No. DMR-1508249. Research conducted at the Spallation Neutron Source (SNS) at Oak Ridge National Laboratory (ORNL) was sponsored by the Scientific User Facilities Division, Office of Basic Energy Sciences, U.S. DOE. This paper was prepared as an account of work sponsored by an agency of the United States Government. Neither the United States Government nor any agency thereof, nor any of their employees, makes any warranty, express or implied, or assumes any legal liability or responsibility for the accuracy, completeness, or usefulness of any information, apparatus, product, or process disclosed, or represents that its use would not infringe privately owned rights. Reference herein to any specific commercial product, process, or service by trade name, trademark, manufacturer, or otherwise does not necessarily constitute or imply its endorsement, recommendation, or favoring by the United

DOI: 10.1021/acs.jpclett.8b01008
J. Phys. Chem. Lett. 2018, 9, 2956−2960

States Government or any agency thereof. The views and opinions of authors expressed herein do not necessarily state or reflect those of the United States Government or any agency thereof.

REFERENCES

(1) Taylor, T. M.; Davidson, P. M.; Bruce, B. D.; Weiss, J. Liposomal nanocapsules in food science and agriculture. *Crit. Rev. Food Sci. Nutr.* **2005**, *45* (7−8), 587−605.

(2) Woodka, A. C.; Butler, P. D.; Porcar, L.; Farago, B.; Nagao, M. Lipid bilayers and membrane dynamics: insight into thickness fluctuations. *Phys. Rev. Lett.* **2012**, *109* (5), 058102.

(3) Nickels, J. D.; Cheng, X.; Mostofian, B.; Stanley, C.; Lindner, B.; Heberle, F. A.; Perticaroli, S.; Feygenson, M.; Egami, T.; Standaert, R. F.; Smith, J. C.; Myles, D. A.; Ohl, M.; Katsaras, J. Mechanical Properties of Nanoscopic Lipid Domains. *J. Am. Chem. Soc.* **2015**, *137* (50), 15772−80.

(4) Yi, X.; Shi, X.; Gao, H. Cellular uptake of elastic nanoparticles. *Phys. Rev. Lett.* **2011**, *107* (9), 098101.

(5) Harland, C. W.; Bradley, M. J.; Parthasarathy, R. Phospholipid bilayers are viscoelastic. *Proc. Natl. Acad. Sci. U. S. A.* **2010**, *107* (45), 19146−50.

(6) Simons, K.; Ikonen, E. Functional rafts in cell membranes. *Nature* **1997**, *387* (6633), 569−72.

(7) Weigel, A. V.; Simon, B.; Tamkun, M. M.; Krapf, D. Ergodic and nonergodic processes coexist in the plasma membrane as observed by single-molecule tracking. *Proc. Natl. Acad. Sci. U. S. A.* **2011**, *108* (16), 6438−43.

(8) Seisenberger, G.; Ried, M. U.; Endress, T.; Buning, H.; Hallek, M.; Brauchle, C. Real-time single-molecule imaging of the infection pathway of an adeno-associated virus. *Science* **2001**, *294* (5548), 1929−32.

(9) Gupta, S.; Biehl, R.; Sill, C.; Allgaier, J.; Sharp, M.; Ohl, M.; Richter, D. Protein Entrapment in Polymeric Mesh: Diffusion in Crowded Environment with Fast Process on Short Scales. *Macromolecules* **2016**, *49* (5), 1941−1949.

(10) He, Y.; Burov, S.; Metzler, R.; Barkai, E. Random time-scale invariant diffusion and transport coefficients. *Phys. Rev. Lett.* **2008**, *101* (5), 058101.

(11) Szymanski, J.; Weiss, M. Elucidating the origin of anomalous diffusion in crowded fluids. *Phys. Rev. Lett.* **2009**, *103* (3), 038102.

(12) Llopis, P. M.; Jackson, A. F.; Sliusarenko, O.; Surovtsev, I.; Heinritz, J.; Emonet, T.; Jacobs-Wagner, C. Spatial organization of the flow of genetic information in bacteria. *Nature* **2010**, *466* (7302), 77−81.

(13) Kolesov, G.; Wunderlich, Z.; Laikova, O. N.; Gelfand, M. S.; Mirny, L. A. How gene order is influenced by the biophysics of transcription regulation. *Proc. Natl. Acad. Sci. U. S. A.* **2007**, *104* (35), 13948−53.

(14) Hoffmann, I.; Michel, R.; Sharp, M.; Holderer, O.; Appavou, M. S.; Polzer, F.; Farago, B.; Gradzielski, M. Softening of phospholipid membranes by the adhesion of silica nanoparticles−as seen by neutron spin-echo (NSE). *Nanoscale* **2014**, *6* (12), 6945−52.

(15) Zilman, A. G.; Granek, R. Undulations and Dynamic Structure Factor of Membranes. *Phys. Rev. Lett.* **1996**, *77* (23), 4788−4791.

(16) Watson, M. C.; Brown, F. L. Interpreting membrane scattering experiments at the mesoscale: the contribution of dissipation within the bilayer. *Biophys. J.* **2010**, *98* (6), L9−L11.

(17) Nagao, M.; Kelley, E. G.; Ashkar, R.; Bradbury, R.; Butler, P. D. Probing Elastic and Viscous Properties of Phospholipid Bilayers Using Neutron Spin Echo Spectroscopy. *J. Phys. Chem. Lett.* **2017**, *8*, 4679−4684.

(18) Takeda, T.; Kawabata, Y.; Seto, H.; Komura, S.; Ghosh, S. K.; Nagao, M.; Okuhara, D. Neutron spin−echo investigations of membrane undulations in complex fluids involving amphiphiles. *J. Phys. Chem. Solids* **1999**, *60* (8−9), 1375−1377.

(19) Mell, M.; Moleiro, L. H.; Hertle, Y.; Fouquet, P.; Schweins, R.; Lopez-Montero, I.; Hellweg, T.; Monroy, F. Bending stiffness of biological membranes: what can be measured by neutron spin echo? *Eur. Phys. J. E: Soft Matter Biol. Phys.* **2013**, *36* (7), 75.

(20) Pencer, J.; Nieh, M. P.; Harroun, T. A.; Krueger, S.; Adams, C.; Katsaras, J. Bilayer thickness and thermal response of dimyristoylphosphatidylcholine unilamellar vesicles containing cholesterol, ergosterol and lanosterol: a small-angle neutron scattering study. *Biochim. Biophys. Acta, Biomembr.* **2005**, *1720* (1−2), 84−91.

(21) Kucerka, N.; Tristram-Nagle, S.; Nagle, J. F. Structure of fully hydrated fluid phase lipid bilayers with monounsaturated chains. *J. Membr. Biol.* **2006**, *208* (3), 193−202.

(22) Tristram-Nagle, S.; Nagle, J. F. HIV-1 fusion peptide decreases bending energy and promotes curved fusion intermediates. *Biophys. J.* **2007**, *93* (6), 2048−55.

(23) Lee, C. H.; Lin, W. C.; Wang, J. All-optical measurements of the bending rigidity of lipid-vesicle membranes across structural phase transitions. *Phys. Rev. E: Stat. Phys., Plasmas, Fluids, Relat. Interdiscip. Top.* **2001**, *64* (2), 020901.

(24) Lee, J. H.; Choi, S. M.; Doe, C.; Faraone, A.; Pincus, P. A.; Kline, S. R. Thermal fluctuation and elasticity of lipid vesicles interacting with pore-forming peptides. *Phys. Rev. Lett.* **2010**, *105* (3), 038101.

(25) Komura, S.; Takeda, T.; Kawabata, Y.; Ghosh, S. K.; Seto, H.; Nagao, M. Dynamical fluctuation of the mesoscopic structure in ternary C12E5-water-n-octane amphiphilic system. *Phys. Rev. E: Stat. Phys., Plasmas, Fluids, Relat. Interdiscip. Top.* **2001**, *63* (4), 041402.

(26) Odeh, F.; Heldt, N.; Gauger, M.; Slack, G.; Li, Y. PFG-NMR Investigation of Liposome Systems Containing Hydrotrope. *J. Dispersion Sci. Technol.* **2006**, *27* (5), 665−669.

(27) Schneider, G. J.; Nusser, K.; Neueder, S.; Brodeck, M.; Willner, L.; Farago, B.; Holderer, O.; Briels, W. J.; Richter, D. Anomalous chain diffusion in unentangled model polymer nanocomposites. *Soft Matter* **2013**, *9* (16), 4336.

(28) Gerstl, C.; Schneider, G. J.; Fuxman, A.; Zamponi, M.; Frick, B.; Seydel, T.; Koza, M.; Genix, A. C.; Allgaier, J.; Richter, D.; Colmenero, J.; Arbe, A. Quasielastic Neutron Scattering Study on the Dynamics of Poly(alkylene oxide)s. *Macromolecules* **2012**, *45* (10), 4394−4405.

(29) Akimoto, T.; Yamamoto, E.; Yasuoka, K.; Hirano, Y.; Yasui, M. Non-Gaussian fluctuations resulting from power-law trapping in a lipid bilayer. *Phys. Rev. Lett.* **2011**, *107* (17), 178103.

(30) Jeon, J.-H.; Javanainen, M.; Martinez-Seara, H.; Metzler, R.; Vattulainen, I. Protein Crowding in Lipid Bilayers Gives Rise to Non-Gaussian Anomalous Lateral Diffusion of Phospholipids and Proteins. *Phys. Rev. X* **2016**, *6* (2), 021006.

(31) Sharma, V. K.; Mamontov, E.; Ohl, M.; Tyagi, M. Incorporation of aspirin modulates the dynamical and phase behavior of the phospholipid membrane. *Phys. Chem. Chem. Phys.* **2017**, *19* (3), 2514−2524.

(32) Flenner, E.; Das, J.; Rheinstadter, M. C.; Kosztin, I. Subdiffusion and lateral diffusion coefficient of lipid atoms and molecules in phospholipid bilayers. *Phys Rev E Stat Nonlin Soft Matter Phys* **2009**, *79* (1), 011907.

(33) Pandey, R. B.; Anderson, K. L.; Farmer, B. L. Multiscale mode dynamics of a tethered membrane. *Phys Rev E Stat Nonlin Soft Matter Phys* **2007**, *75* (6), 061913.

(34) Mangiapia, G.; Gvaramia, M.; Kuhrts, L.; Teixeira, J.; Koutsioubas, A.; Soltwedel, O.; Frielinghaus, H. Effect of benzocaine and propranolol on phospholipid-based bilayers. *Phys. Chem. Chem. Phys.* **2017**, *19* (47), 32057−32071.

(35) Katsaras, J.; Gutberlet, T. *Lipid Bilayers: Structure and Interactions*; Springer-Verlag: Berlin, 2001.

DOI: 10.1021/acs.jpclett.8b01008
J. Phys. Chem. Lett. 2018, 9, 2956−2960